Photorefractive Properties of Poly(*N*-vinyl carbazole)-Based Composites for High-Speed Applications

M. A. Díaz-García,† D. Wright, J. D. Casperson, B. Smith, E. Glazer, and W. E. Moerner*,‡

Department of Chemistry, University of California San Diego, La Jolla, California 92093-0340

L. I. Sukhomlinova and R. J. Twieg*

Department of Chemistry, Kent State University, Kent, Ohio 44242

Received December 30, 1998. Revised Manuscript Received April 29, 1999

The photorefractive properties of polymer composites based on poly(*N*-vinylcarbazole), doped with the sensitizer C_{60}, the plasticizer butyl benzyl phthalate, and two series of chromophores are presented. The influence of the structure and the oxidation potential of the chromophore on the photorefractive properties is discussed. These materials show promise for video-rate optical processing applications, since they exhibit fast response times (beam-coupling growth times, τ_g, as small as 60 ms at 50 V/μm applied field and 200 mW/cm^2 intensity and τ_g as small as 5 ms at 100 V/μm and 1 W/cm^2).

Introduction

The past 30 years have produced extensive research on the properties of photorefractive (PR) materials, mainly motivated by the wide range of potential applications for which they can be used (e.g. optical processing, phase conjugation, optical storage, and many others).[1,2] The early work focused exclusively on inorganic crystalline materials, such as $LiNbO_3$, and many applications were demonstrated at the proof-of-principle level. In 1991, a major step forward was achieved when photorefractivity was demonstrated in polymers,[3] since it became possible to separately optimize the individual components necessary for photorefractivity in low-cost samples not requiring careful crystal growth. Although the performance of the first materials was relatively poor [gain coefficients (Γ) $\sim$ 1 cm^{-1}, no net gain, diffraction efficiencies (η) $\sim 10^{-6}$, and grating growth times (τ_g) of many minutes at 1 W/cm^2], progress in material performance occurred rapidly.[4] Critical milestones included the achievement of net gain,[5] overmodulated η, subsecond response times, and Γ values in the 100−200 cm^{-1} range.[6,7] The two underlying reasons for this high performance have been shown to be (a) an orientational enhancement of the nonlinearity resulting from the low glass transition temperature[8] and (b) high values of the space-charge field resulting from the large trap densities[9,10] and the relatively low dielectric constant of polymers compared to the inorganic crystals.

As a result of the discovery of the orientational enhancement mechanism in these low T_g systems, the design of the chromophores for photorefractivity has diverged from the original electrooptic chromophores that were first employed. Recent work has concentrated on a simple figure-of-merit expression for photorefractive chromophores,[11] which can be written as[12]

$$F = \frac{9\mu_g\beta}{M} + \frac{2\mu_g{}^2\Delta\alpha}{kTM} \qquad (1)$$

where μ_g is the ground-state dipole moment, β is the

† Present address: Departamento Ciencia y Tecnología, Universidad Miguel Hernández, Elche-03202, Alicante, Spain.

‡ Present address: Department of Chemistry, Stanford University, Stanford, CA 94305-5080.

(1) Günter, P.; Huignard, J.-P. *Photorefractive Materials and Their Applications I and II*; Springer-Verlag: Berlin, 1988.

(2) Solymar, L.; Webb, D. J.; Grunnet-Jepsen, A. *The Physics and Applications of Photorefractive Materials*; Clarendon Press: Oxford, 1996.

(3) Ducharme, S.; Scott, J. C.; Twieg, R. J.; Moerner, W. E. *Phys. Rev. Lett.* **1991**, *66*, 1846.

(4) Moerner, W. E.; Silence, S. M. *Chem. Rev.* **1994**, *94*, 127.

(5) Donckers, M. C. J. M.; Silence, S. M.; Walsh, C. A.; Hache, F.; Burland, D. M.; Moerner, W. E.; Twieg, R. J. *Opt. Lett.* **1993**, *18*, 1044.

(6) Meerholz, K.; Volodin, B. L.; Sandalphon; Kippelen, B.; Peyghambarian, N. *Nature* (*London*) **1994**, *371*, 497.

(7) (a) Moerner, W. E.; Grunnet-Jepsen, A.; Thompson, C. L. *Annu. Rev. Mater. Sci.* **1997**, *27* 585. (b) Würthner, F.; Wortmann, R.; Matchiner, R.; Lukaszuk, K.; Meerholz, K.; DeNardin, Y.; Bittner, R.; Brauchle, C.; Sens, R. *Angew. Chem., Int. Ed. Engl.* **1997**, *36*, 2765. (c) Kippelen, B.; Marder, S. R.; Hendrickx, E.; Maldonado, J. L.; Guilemet, G.; Volodin, B. L.; Steele, D. D.; Enami, Y.; Sandalphon; Jao, Y. J.; Wang, J. F.; Röckel, H.; Erskine, L.; Peyghambarian, N. *Science* **1998**, *279*, 54.

(8) Moerner, W. E.; Silence, S. M.; Hache, F.; Bjorklund, G. C. *J. Opt. Soc. Am. B* **1994**, *11*, 320.

(9) Grunnet-Jepsen, A.; Wright, D.; Smith, B.; Bratcher, M. S.; DeClue, M. S.; Siegel, J. S.; Moerner, W. E. *Chem. Phys. Lett.* **1998**, *291*, 553.

(10) Grunnet-Jepsen, A.; Thompson, C. L.; Moerner, W. E. *J. Opt. Soc. Am. B* **1998**, *15*, 905.

(11) (a) Wortmann, R.; Poga, C.; Twieg, R. J.; Geletneky, C.; Moylan, C. R.; Lundquist, P. M.; DeVoe, R. G.; Cotts, P. M.; Horn, H.; Rice, J. E.; Burland, D. M. *J. Chem. Phys.* **1996**, *105*, 10637. (b) Kipplen, K.; Meyers, F.; Peyghambarian, N.; Marder, S. *J. Am. Chem. Soc.* **1997**, *15*, 9929. (c) Moylan, C. R.; Wortmann, R.; Twieg, R. J.; McComb, I. *J. Opt. Soc. Am. B.* **1998**, *15*, 929.

(12) This expression essentially results from expressing the *C* coefficient in ref 8 in the form appropriate for the two-level approximation and the oriented gas model.

10.1021/cm981157h CCC: $18.00 © 1999 American Chemical Society
Published on Web 06/16/1999

first hyperpolarizability, M is the molar mass, k is Boltzmann's constant, T is the temperature, and $\Delta\alpha = \alpha_{\parallel} - \alpha_{\perp}$ is the polarizability anisotropy, i.e., the difference in optical polarizability parallel and perpendicular to the molecular axis. In most of the molecules studied to date, the second term on the right-hand side in eq 1 has been dominant. Thus, rather than seeking chromophores that possess large first hyperpolarizability, efforts are now underway to find new chromophores which possess instead a large linear polarizability anisotropy. Also, as a result of the μ_g^2 factor in the second term on the right-hand side, the emphasis on large ground-state dipole moment is even more important in these new chromophores than in the case of the electrooptic-based systems.

In contrast with the improvements in gain and diffraction efficiency, relatively few advances have occurred in the speed of grating formation in PR polymers, with most materials showing grating growth times in the range 0.1−100 s at the canonical 1 W/cm^2 writing intensity. One exception to this was a composite denoted PTPDac-BA2/DEANST/C_{60}, which showed a response time as low as 7.5 ms at 0.25 W/cm^2.[13] However, the net gain coefficient Γ was only 33.5 cm^{-1}. Very recently, we reported several high-speed PR composites with growth times less than 10 ms at 1 W/cm^2, while high net gain coefficients were maintained (>100 cm^{-1}), thus opening new possibilities for video-rate optical processing applications.[14] For example, a polymer composite denoted PVK:AODCST:BBP:C_{60} has shown a grating growth time as small as 5 ms at 100 V/μm applied electric field and a net gain coefficient Γ > 200 cm^{-1}.[14] In this material, the host polymer PVK (poly(*N*-vinylcarbazole)) is doped with the nonlinear optical chromophore AODCST, the plasticizer butyl benzyl phthalate (BBP), and the sensitizer C_{60}.

In this paper we investigate the photorefractive properties of materials of the general composition PVK:chromophore:BBP:C_{60}, where only the chromophore structure changes. Two series of chromophores are described: a series of dicyanostyrene (DCST) derivatives with varying amine donor, including the previously reported PDCST, AODCST, and TDDCST, and a series of cyano ester styrene (CEST) derivatives with varying amine donor. The effect of the structure and oxidation potential of the chromophore on the PR properties is discussed, with particular emphasis on the speed of formation of two-beam-coupling gain.

There are numerous reasons for examination of these new CEST derivatives in addition to the DCST derivatives. The main impetus here is the need to simultaneously optimize the electronic and optical properties of the chromophores (including the ground-state dipole moment, birefringence, oxidation potential, and first hyperpolarizability) alongside important ancillary properties related to processing and sample stability (miscibility, loading, phase separation, etc.) which may be provided by the various functional groups. As will be seen (by comparison of Tables 1 and 2, vide infra), the cyano ester materials presently appear to offer no specific or overall benefits relative to the dicyano derivatives. In particular, there was no case of enhancement in either two-beam coupling efficiency or response speed when these two classes are compared, with C_{60} as the sensitizer and PVK as the transport agent.

(13) Ogino, K.; Nomura, T.; Shichi, T.; Park, S.; Sato, H.; Aoyama, T.; Wada, T. *Chem. Mater.* **1997**, *9*, 2768.

(14) Wright, D.; Diaz-Garcia, M. A.; Casperson, J. D.; DeClue, M.; Moerner, W. E.; Twieg, R. J. *Appl. Phys. Lett.* **1998**, *73*, 1490.

Experimental Section

Synthesis. Representative synthetic procedures follow.

4-[Bis(2-methoxyethyl)amino]benzaldehyde. A solution of 4-fluorobenzaldehyde (12.41 g, 0.1 mol) and bis(2-methoxyethyl)amine (39.96 g, 0.3 mol) in DMSO (70 mL) was heated at 170 °C for 8 h under nitrogen. The resulting brown solution was diluted with water (250 mL) and extracted with ethyl acetate (4 × 100 mL). The combined organic extracts were washed with water, and dried over $MgSO_4$, and the solvent was concentrated in vacuo. The resulting crude product was purified by column chromatography (eluent, ethyl acetate−petroleum ether mixture, 1:6) to afford 12 g (50%) of 4-bis(2-methoxyethyl)aminobenzaldehyde as an oil. ^{1}H NMR (300 MHz, $CDCl_3$) δ: 9.72 (s, 1H), 7.70 (d, J = 8.7 Hz, 2H), 6.75 (d, J = 8.7 Hz, 2H), 3.66 (t, J = 6.3 Hz, J = 5.7 Hz, 4H), 3.57 (t, J = 5.4 Hz, 4H), 3.35 (s, 6H). ^{13}C NMR (75 MHz, $CDCl_3$) δ: 50.82, 58.82, 69.68, 110.88, 125.18, 131.86, 152.50, 189.8.

2-[4-Bis(2-methoxyethyl)amino]benzylidene]malononitrile (AODCST). To a solution of 4-bis(2-methoxyethyl)-aminobenzaldehyde (10 g, 0.042 mol) and malononitrile (3.06 g, 0.046 mol) in *n*-PrOH (70 mL) was added a catalytic amount of piperidine. The reaction mixture was heated to boiling and then cooled to room temperature. The product was filtered and recrystallized from methanol to give 8 g (67%) of AODCST as yellow crystals, mp 83−84 °C. ^{1}H NMR (300 MHz, $CDCl_3$) δ: 7.79 (d, J = 9 Hz, 2H), 7.45 (s, 1H), 6.76 (d, J = 9 Hz, 2H), 3.69 (t, J = 5.7 Hz, 4H), 3.58 (t, J = 5.7 Hz, 4H), 3.35 (s, 6H). ^{13}C NMR (75 MHz, $CDCl_3$) δ: 51.00, 58.95, 69.73, 111.78, 114.68, 115.75, 119.37, 133.70, 152.94, 157.72.

2-Cyano-3-[4-[bis(2-methoxyethyl)amino]phenyl]acrylic Acid 2-Methoxyethyl Ester (CEST 7). A solution of 4-[bis-(2-methoxyethyl)amino]benzaldehyde (2.4 g, 0.01 mol), 2-methoxyethyl cyanoacetate (1.72 g, 0.012 mol), and a catalytic amount of piperidine in n-PrOH (10 mL) was refluxed for 2 h. The solvent was concentrated under vacuum and the resulting crude product was purified by column chromatography (eluent ethyl acetate−petroleum ether mixture, 1:4) to afford 2.2 g (60%) of 2-cyano-3-[4-[bis(2-methoxyethyl)amino]phenyl]acrylic acid 2-methoxyethyl ester as an oil. ^{1}H NMR (300 MHz, $CDCl_3$) δ: 8.07 (s, 1H), 7.91 (d, J = 9 Hz, 2H), 6.76 (d, J = 9 Hz, 2H), 4.43 (t, J = 4.5 Hz, 2H), 3.72−3.58 (m, 10H), 3.43 (s, 3H), 3.35 (s, 6H). ^{13}C NMR (75 MHz, $CDCl_3$) δ: 50.79, 58.77, 64.57, 69.65, 69.97, 93.61, 111.44, 116.99, 119.26, 133.91, 151.97, 154.18, 163.88.

This standard procedure can be used for the synthesis of cyano ester styrene derivatives. However, transesterification can take place under such reaction conditions and the appropriate alcohol should be used as a solvent. For example, the reaction of 4-(diethylamino)benzaldehyde with 2-methoxyethyl cyanoacetate in refluxing propanol afforded both 2-cyano-3-[4-(diethylamino)phenyl]acrylic acid 2-methoxyethyl ester (**CEST-2**) and 2-cyano-3-[4-(dimethylamino)phenyl]-acrylic acid propyl ester (**CEST-1**).

2-Cyano-3-[4-(diethylamino)phenyl]acrylic Acid Propyl Ester (CEST 1). ^{1}H NMR (300 MHz, $CDCl_3$) δ: 8.05 (s, 1H), 7.92 (d, J = 8.7 Hz, 2H), 6.69 (d, J = 8.7 Hz, 2H), 4.23 (t, J = 6.9 Hz, 2H), 3.45 (q, J = 6.9 Hz, 4H), 1.77 (sextet, J = 7.2 Hz, 2H), 1.23 (t, J = 6.9 Hz, 6H), 1.01 (t, J = 7.2 Hz, 3H). ^{13}C NMR (75 MHz, $CDCl_3$) δ: 10.24, 12.37, 21.94, 44.83, 67.22, 93.20, 111.36, 117.47, 119.20, 134.22, 151.18, 154.12, 164.33. Mp: 87−89 °C.

2-Cyano-3-[4-(diethylamino)phenyl]acrylic Acid 2-Methoxyethyl Ester (CEST 2). ^{1}H NMR (300 MHz, $CDCl_3$) δ: 8.05 (s, 1H), 7.92 (d, J = 9 Hz, 2H), 6.68 (d, J = 9 Hz, 2H), 4.42 (t, J = 4.8 Hz, 2H), 3.70 (t, J = 4.5 Hz, 2H), 3.49−3.42 (m, 7H), 1.22 (t, J = 6.9 Hz, 6H). ^{13}C NMR (75 MHz, $CDCl_3$) δ: 12.38,

Table 1. Photorefractive Properties of Composites of (PVK:Chromophore:BBP:C_{60}) for Different DCST Chromophores[a]

DCST	Chemical Structure	α (cm^{-1})	σ_{ph} (pS/cm)	σ_d (pS/cm)	Γ (cm^{-1})	Δn (10^{-3})	τ_g (s)	σ_{ph}/α (pS/cm)	τ_g^{-1}/α (cm/s)
MPDCST	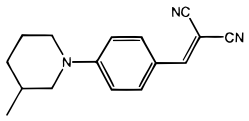	11.0	1.7	0.039	67	0.62	0.251 ±0.001	0.158	0.362
PDCST	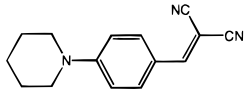	14.1	3.5	0.077	73	0.57	0.196 ±0.006	0.248	0.362
TDDCST	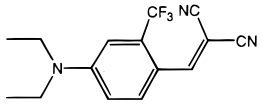	8.5	2.0	0.045	62	0.52	0.322 ±0.030	0.235	0.365
7-DCST	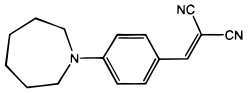	26.2	9.2	0.021	38	0.43	0.059 ±0.003	0.351	0.647
DDCST	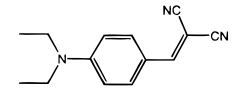	19.4	7.5	0.085	63	0.49	0.078 ±0.015	0.384	0.636
AODCST	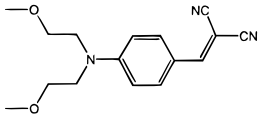	9.0	6.9	0.050	80	0.59	0.096 ±0.003	0.743	1.154

[a] σ_{ph} (photoconductivity) and σ_d (dark conductivity) were obtained at 20 V/μm and 200 mW/cm²; α (absorption coefficient); Γ (gain coefficient), τ_g (response time), and Δ*n* (refractive index change) were obtained at 647 nm, 50 V/μm, and 200 mW/cm².

44.69, 59.04, 64.68, 70,17, 92.89, 111.15, 117.41, 118.80, 134.36, 151.50, 154.43, 164.31. Mp: 62−63 °C.

Sample Preparation. A detailed description of the sample preparation procedure can be found elsewhere.[10,15] Solutions containing the hole-transporting polymer poly(*N*-vinylcarbazole) (PVK) (49.5 wt %), chromophore (one of the DCST or CEST derivatives) (35 wt %), the liquid plasticizer butyl benzyl phthalate (BBP) (15 wt %), and the sensitizer C_{60} (0.5 wt %) were prepared in chlorobenzene. The solutions were then cast at 45 °C onto indium−tin oxide (ITO) coated glass plates and dried overnight in an oven at a temperature ranging between 70 and 130 °C (depending on the melting point of the chromophore). Finally, the plates were assembled at a temperature around 10 °C above the drying temperature, yielding films of thickness between 80 and 130 μm. Teflon spacers were used to ensure a uniform thickness.

Optical Experiments. Absorption coefficients were obtained for each sample on a Lambda 19 absorption spectrometer. The photoconductivity experiments were performed by a simple DC technique.[15] A field of 20 V/μm was applied to the sample in the dark and during illumination at 647 nm, with an intensity of 200 mW/cm². The measurement of the current flowing through the sample in both cases permitted the determination of the dark conductivity (σ_d) and the photoconductivity (σ_{ph}).

Standard two-wave-mixing experiments[10] were performed at 647 nm. Two p-polarized beams of equal intensity intersected the sample in a tilted geometry configuration, with external angles of 30 and 60° with respect to the sample normal. The transmitted output powers where then monitored. The experiment was performed by the following procedure: first, to check for the presence of beam fanning,[7a,16] a DC electric field was applied to the sample, the pump beam turned on for 1 s and its transmitted power monitored. Then, with the DC field still present, both beams were turned on and their powers monitored with respect to time, until steady-state energy transfer was achieved. Time constants were obtained from these transients by using a fitting function as described in detail below. The gain coefficient (Γ) was determined from the measurement of the multiplicative gain factor (γ) at steady state. After a few seconds at steady state, the optical interference pattern was translated at a speed much faster than the response time of the material, by moving a mirror in the pump beam path with a piezoelectric actuator. The resulting power oscillations were used to obtain the maximum index modulation (Δ*n*) and the phase shift (ϕ).

Cyclic Voltammetry. All electrochemical experiments were conducted using a BAS CV-50W Voltammetric Analyzer, with Pt working and auxiliary electrodes. Samples were prepared in concentrations of 5×10^{-3} M in degassed acetonitrile solutions containing 0.1 M Bu_4NPF_6 (TBAH), and potentials were measured vs a $Ag/AgNO_3/CH_3CN$ reference electrode. Peak potentials were obtained from square wave voltammograms. Ferrocene was used as a calibration standard, and under these conditions the $E_{1/2}$ value was 0.122 V for the Fc/Fc^+ couple.

(15) Grunnet-Jepsen, A.; Thompson, C. L.; Twieg, R. J.; Moerner, W. E. *Appl. Phys. Lett.* **1997**, *70*, 1515.

(16) (a) Grunnet-Jepsen, A.; Thompson, C. L.; Twieg, R. J.; Moerner, W. E. *J. Opt. Soc. Am. B* **1998**, *15*, 901. (b) Meerholz, K.; Bittner, R.; De Nardin, Y. *Opt. Comm.* **1998**, *150*, 205.

Table 2. Photorefractive Properties of Composites of (PVK:Chromophore:BBP:C_{60}) for Different CEST Chromophores[a]

CEST	Chemical Structure		α (cm^{-1})	σ_{ph} (pS/cm)	σ_d (pS/cm)	Γ (cm^{-1})	Δn (10^{-3})	τ_g (s)	σ_{ph}/α (pS)	τ_g^{-1}/α (cm/s)
	R_1	R_2								
1	C_2H_5	C_3H_7	13.0	1.2	0.081	37	0.39	0.26 ±0.01	0.09	0.26 ±0.02
2	C_2H_5	$CH_2CH_2OCH_3$	16.0	0.8	0.143	44	0.34	0.20 ±0.01	0.5	0.71 ±0.05
3	C_2H_5	C_8H_{17}	12.0	1.8	0.120	36	0.29	0.10 ±0.02*	0.15	0.8 ±0.3*
4	C_2H_5	C_4H_9	12.0	1.7	0.124	29	0.30	0.16 ±0.01	0.15	0.52 ±0.03
5	C_2H_5	$C(CH_3)_3$	16.6	1.4	0.016	13	0.15	0.10 ±0.02	0.08	0.58 ±0.08
6	C_2H_5	CH_3	21.0	2.2	0.026	36	0.46	0.09 ±0.01	0.10	0.51 ±0.03
7	$CH_3OCH_2CH_2$	$CH_2CH_2OCH_3$	13.8	0.8	0.154	8	0.15	0.16 ±0.05	0.06	0.5 ±0.1
8	CH_3	$CH_2CH_2OCH_3$	10.5	1.5	0.126	22	0.30	0.06 ±0.01*	0.14	1.6 ±0.4*

[a] σ_{ph} (photoconductivity) and σ_d (dark conductivity) were obtained at 20 V/μm and 200 mW/cm^2; α (absorption coefficient), Γ (Gain coefficient), τ_g (response time), and Δn (refractive index change) were obtained at 647 nm, 50 V/μm, and 200 mW/cm^2. *Error was estimated from measurements on several samples prepared from different solutions, while in the rest of the cases it was obtained from measurements on several samples prepared from the same solution.

Scheme 1. Synthetic Route to Dicyanostyrene (DCST) and Cyano Ester Styrene (CEST) Derivatives[a]

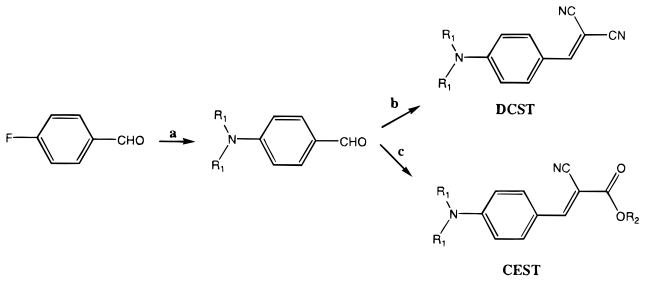

[a] Reagents and conditions: (a) $(R_1)_2NH$, DMSO or NMP, 100−180 °C; (b) $CH_2(CN)_2$, *n*-PrOH, $C_5H_{11}N$ catalyst; (c) $NCCH_2CO_2R_2$, *n*-PrOH, $C_5H_{11}N$ catalyst.

Results and Discussion

To provide a range of photorefractive chromophores, DCST and CEST derivatives have been synthesized by the condensation of malononitrile or alkyl cyanoacetate with corresponding aldehydes (Scheme 1, see the Experimental Section). The condensation of aromatic aldehydes with cyanoacetic esters has been shown[17] to afford only trans isomers of cyano ester styrenes. The chemical structures of all compounds of both series are shown in Tables 1 and 2 for the DCSTs and CESTs, respectively.

The photorefractive properties were investigated by standard two-wave-mixing (TWM) experiments to measure the dynamics of the two-beam-coupling gain as described in the Experimental Section.[4,10] This method has the advantage that the observation of asymmetric two-beam-coupling in an optically thick sample is an unambiguous signature of photorefractivity and not some local photophysical or photochemical effect producing index modulation. By fitting the two-wave-mixing transients with a growth function, the speed of the effect can be quantified. In the simplest single-carrier model of photorefractivity the gain growth transients are exponential.[1,2,18] This result is valid under several approximations, including small charge modulation, negligible absorption, weak energy transfer, nondispersive charge mobility, and the slowly varying amplitude approximation. When these assumptions are not valid, deviations from single-exponential behavior can be expected. One outcome if some of these assumptions are violated is that the recorded grating has a

(17) Hayashi, T. *J. Org. Chem*. **1966**, *31*, 3253.
(18) Kukhtarev, N. V.; Markov, V. B.; Odulov, S. G.; Soskin, M. S.; Vinetskii, V. L. *Ferroelectrics* **1979**, *22*, 949; **1979**, *22*, 961.

nonsinusoidal shape that distorts the long-time growth transient away from the exponentially growing form.[1] This problem has been usually circumvented by interpreting only the short-time constant, while the grating is still approximately sinusoidal. In some of the materials reported in this work, the nonexponential behavior of the grating growth has been observed, probably due to violations of the assumptions of weak energy transfer and nondispersive mobility. A detailed study of the cause of the nonexponential transients is out of the scope of this paper, so we simply report time constants characteristic of the early-time growth derived from simple fitting functions which allows a relative comparison of the different materials.

Samples of the type PVK:chromophore:BBP:C_{60} were prepared for the various chromophores, following the method described in the Experimental Section. Samples showed good optical clarity and did not undergo degradation due to crystallization for at least 6 months. The DCST derivatives appear to be very stable, with reproducible performance over the time period investigated. On the other hand, some of the CESTs seemed to yield less stable samples. In particular, CESTs **1** and **8** showed slight changes in color in the edges after 1 month, perhaps due to water vapor absorption. Fortunately, this problem can be easily solved by hermetically sealing the samples.

TWM experiments were performed at a laser wavelength of 647 nm (see the Experimental Section), where essentially all the optical absorption is due to the C_{60} sensitizer and not to the chromophores (typical wavelength of maximum absorption $\lambda_{max} \sim 428$ nm for the CESTs and $\lambda_{max} \sim 435$ nm for the DCSTs). Therefore, the absorption coefficients at 647 nm provide a trivial way to determine the precise content of C_{60} in the samples. This is an important issue which needs to be considered for a valid comparison of the different chromophores (vide infra).

In Tables 1 and 2 we report the photorefractive properties of the composites based on the DCST and CEST derivatives, respectively, from TWM experiments performed at low applied electric fields (20 and 50 V/μm for PC and TWM respectively) and low writing intensities (sum of writing beam intensities 200 mW/cm^2). Absorption coefficients at 647 nm, photo and dark conductivities, gain coefficients, and maximum index modulations were determined. For the low field and intensity data, one time constant, τ_g, was obtained by fitting the evolution of the growth of the gain with a single-exponential function of the form

$$\gamma(t) = 1 + \gamma_0\{1 - \exp[-(t/\tau_g)]\} \qquad (2)$$

where γ_0 is the steady-state gain. The same values of τ_g were obtained when fitting only the early growth or when fitting the complete curve until steady state was reached. This indicates that with these experimental conditions the distortion of the transient by the various complicating effects mentioned earlier were negligible.

It should be noted that although samples were prepared by adding a nominal 0.5 wt % of C_{60} to the sample mixture, the absorption coefficients vary from one sample to another. Both the photoconductivity (σ_{ph}) and the speed (τ_g^{-1}) are proportional to the rate of generation of mobile charges in the material and, therefore, to the absorption. Consequently, to compare the performance of the different chromophores, we normalize both the photoconductivity and speed by dividing by the absorption coefficient of the sample. This ensures that the possible differences observed are not due to a different degree of charge generation caused simply by a different actual doping level of sensitizer. These normalized parameters are also reported in Tables 1 and 2.

Overall, the most important result obtained is that these composites show very fast response times, as compared to other polymer composites previously reported, while high gain coefficients are maintained. Comparing DCSTs to CESTs, with a few exceptions, the photoconductivity and the speed are both higher in the DCST class. In addition, the steady-state gain coefficients are generally larger for the DCSTs than for the CESTs. This difference is probably due to the enhanced ground-state dipole moment of the DCST molecules relative to the CEST molecules. The reported[19,20] values of dipole moment of some DCST molecules [9.16 D for 2-[4-(dimethylamino)benzylidene]malononitrile; 9.0 D for 2-[4-(piperidin-1-ylphenylazo)benzylidene]malononitrile] appear to be larger than for CEST molecules [5.61 D for 2-cyano-3-[4-(dimethylamino)phenyl]acrylic acid ethyl ester; 5.7 D for 2-cyano-3-[4-(4-piperidin-1-ylphenylazo)phenyl]acrylic acid ethyl ester]. Other differences may be due to differences in β or $\Delta\alpha$, but measurement of these molecular quantities is out of the scope of this paper.

Turning to the speed characteristics, since the overall gain coefficient depends on the product of the effective optical nonlinearity and the imaginary part of the space-charge field, there are two physical processes that might be limiting the speed (τ_g^{-1}): the rate of formation of the internal space charge field (E_{sc}) and molecular orientation in response to the local electric field. The first step in the photorefractive effect is the formation of an internal field as a consequence of generation and separation of charges over distances the order of the grating wavelength (here 1.7 μm). The speed of this process further depends on several factors, in particular, charge generation, transport, and trapping effects, that are reflected in the value of the photoconductivity (σ_{ph}). In the simplest model

$$\sigma_{ph} = ne\mu = (\phi\alpha I\tau_t/h\nu)e\mu \qquad (3)$$

where n is the density of carriers, e is the elementary charge, μ is the mobility, ϕ is the charge generation quantum efficiency, α is the absorption coefficient, I is the optical intensity, τ_t is the time constant for transport, h is Planck's constant, and ν is the frequency of the light. The photoconductivity appears as an overall leading factor in the speed of formation of the space-charge field (as long as σ_{ph} is larger than the dark conductivity).[1,2]

Next we consider the formation of an index grating via the dependence of the index of refraction on the local electric field. This process can take place via two

(19) Rivet-Le Guellec, P.; Martin, G. *C. R. Acad. Sci. Paris, Ser. C* **1967**, *265*, 888.
(20) Tirelli, N.; Altomare, A.; Solaro, R.; Ciardelli, F.; Meier, U.; Bosshard, C.; Gunter, P. *J. Prakt. Chem.* **1998**, *340*, 122.

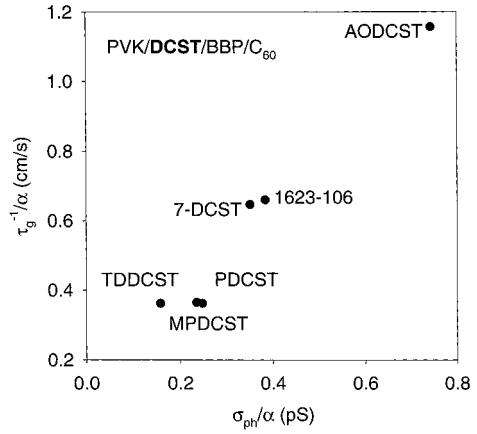

Figure 1. Normalized photorefractive speed (τ_g^{-1}/α) versus normalized photoconductivity (σ_{ph}/α) for composites of PVK/DCST/BBP/C_{60} for different DCST derivatives. α = absorption coefficient.

effects: First, these materials show a Pockels electrooptic nonlinearity due to poling of the chromophores by the uniform applied field, which results in an instantaneous (in response to E_{sc}) index change. Second, in the orientational enhancement model,[8] an additional index modulation occurs due to periodic poling of the chromophores under the *total* local field (applied field + E_{sc}). This latter effect is present in composites with glass transition temperatures near room temperature, such as the present composites. The resulting index change occurs as fast as each chromophore molecule can reorient in response to the local field at the position of the molecule, a process which may be slower or faster than the formation of E_{sc}.

Measurements of the intensity dependence of the response time provide a way to experimentally determine whether the speed is limited by E_{sc} formation or by chromophore orientation. The speed of E_{sc} formation should have the same intensity dependence as the photoconductivity, while the speed of chromophore reorientation has no known intensity dependence. Recently, a preliminary study of this type was reported for composites based on the AODCST chromophore.[14] It was observed that both parameters (τ_g^{-1} and σ_{ph}) grew linearly with intensity without saturation, suggesting that the speed was determined by σ_{ph} and therefore E_{sc} formation. This argument is also supported by the data reported in this work for the DCST derivatives (see Table 1) and is also illustrated in Figure 1, where we plot the normalized PR speed (τ_g^{-1}/α) versus the normalized photoconductivity (σ_{ph}/α). Clearly, one observes the trend of higher speed (τ_g^{-1}/α) with larger photoconductivity (σ_{ph}/α) for all the composites in this class.

The deeper issue of the reason for the different photoconductivities for the different chromophores may be examined by utilizing the results from a previous study of trapping dynamics in C_{60}-doped PR polymers.[9] By utilizing near-infrared spectroscopy of the C_{60} anion in two composites with PDCST and AODCST chromophores, we concluded that the active trap is the C_{60} anion and that charge neutrality is maintained by compensating sites. When the HOMO (highest occupied molecular orbital) of the chromophore is higher than that for the transporting states of PVK (as estimated by the HOMO of *N*-ethylcarbazole[9]), the chromophore

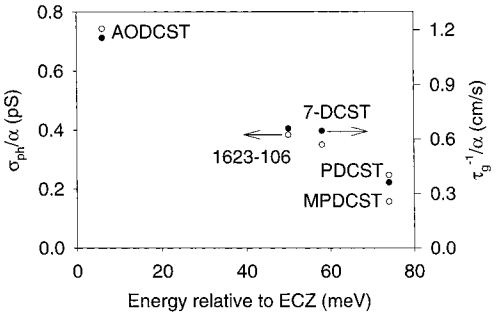

Figure 2. Normalized photorefractive speed (τ_g^{-1}/α) (right axis, filled circles) and normalized photoconductivity (σ_{ph}/α) (left axis, open circles) versus energy position of the HOMO of the chromophore relative to that for ECZ for composites of PVK/DCST/BBP/C_{60} for different DCST derivatives.

acts as the compensator, trapping holes produced by irradiation of the C_{60}. This compensation process results in the formation of the cation of the chromophore. Thus, the depth of the chromophore (HOMO) as a hole trap can affect the available concentration of C_{60} anion. The relative positions of the HOMO of the chromophores were estimated by cyclic voltammetry to measure the oxidation potential. PDCST was determined to have a smaller oxidation potential and was shown to act as a deeper trap for holes than AODCST.

For the purposes of this paper, we can take this model one step further. The key idea is that the role of chromophores acting as (compensating) traps for holes should affect the charge mobility, which in turn effects the photoconductivity (via eq 3), with lower mobility/photoconductivity for deeper hole traps. This behavior has been observed in simulations[21] and experiments[21−24] in which polymers doped with hole[21−23] and electron[24] transport agents were additionally doped with trapping agents. Thus, if the chromophores act as traps in these composites, then the trap depth of the chromophore should govern the mobility. This argument assumes that only the oxidation potential and no other property of the chromophores that could affect the mobility (eg. dipole moment[25]) is changing in the series of chromophores studied.

To test this idea, we performed cyclic voltammetry on all the chromophores and used the first oxidation potentials to locate the relative energy of the HOMO of the chromophore relative to that for *N*-ethylcarbazole (ECZ). Figure 2 shows the results of this analysis, with the left ordinate being the normalized photoconductivity, the right ordinate the normalized speed, and the abscissa the position of the HOMO of the chromophore. This figure shows a very strong trend for the DCST derivatives: the higher (σ_{ph}/α) and (τ_g^{-1}/α) values occur for the most shallow hole trap represented by the presence of the chromophore. For chromophores with smaller oxidation potential (i.e., higher energy relative to ECZ), the traps added by the chromophore are deeper

(21) Wolf, U.; Bässler, H.; Borsenberger, P. M.; Gruenbaum, W. T. *Chem. Phys.* **1997**, *222*, 259.
(22) Veres, J.; Juhasz, C. *Philos. Mag. B* **1998**, *75*, 377.
(23) Borsenberger, P. M.; Gruenbaum, W. T.; Wolf, U.; Bässler, H. *Chem. Phys.* **1998**, *234*, 277.
(24) Borsenberger, P. M.; Gruenbaum, W. T.; Magin, E. H.; Visser, S. A. *Phys. Stat. Sol.* **1998**, *166*, 835.
(25) Goonesekera, A.; Ducharme, S. D. *J. Appl. Phys.* **1999**, *85*, 6506.

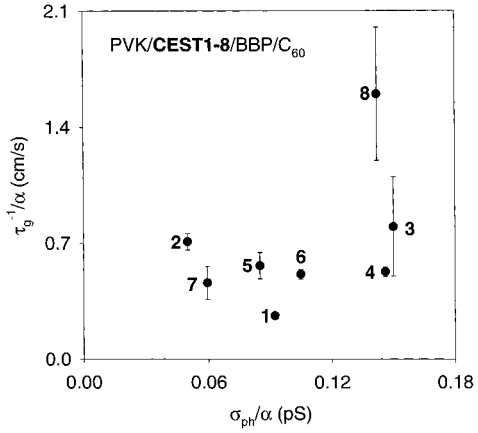

Figure 3. Normalized photorefractive speed (τ_g^{-1}/α) versus normalized photoconductivity (σ_{ph}/α) for composites of PVK/CEST/BBP/C_{60} for different CEST derivatives. α = absorption coefficient. Solid lines are linear regression fits to the data. The error bars represent repetitive measurements on different samples from the same solution (CESTs **2**, **4**−**7**) and different samples from different solutions (CESTs **3** and **8**).

and the transport is hindered. These results give a clear prescription for high-speed performance in this class of materials: the depth of the hole trap provided by the chromophore should be as small as possible relative to that of the primary transport agent.

Turning now to the CEST derivatives, the correlation between (τ_g^{-1}/α) and (σ_{ph}/α) is not so clear (see Figure 3); indeed only small changes in speed are observed from one chromophore to another for almost all cases. First, similar values of (τ_g^{-1}/α) and (σ_{ph}/α) were obtained for CESTs **1**, **3**, **4**, and **6**, which have the same electron donor R_1 structures but different acceptors R_2, differing by an aliphatic chain of different length. Comparing CESTs **2** and **7** with the same acceptor, the change in the donor from the diethylamine to bis(2-methoxyethyl)-amine produces almost no change in speed or photoconductivity. On the other hand, the change of R_1 in CEST **8** compared to CEST **1**−**6** leads to a faster response, while a similar σ_{ph} value is maintained. These results indicate that the PR performance of these materials can be altered in some cases by changing R_1, while it is practically insensitive to changes of R_2.

To obtain further insight into the CEST materials, we performed intensity dependent studies of (τ_g^{-1}/α) and (σ_{ph}/α) for CESTs **3** and **8**, which have similar (σ_{ph}/α) but strangely differ in speed. Figure 4a shows the results obtained for the fastest material, CEST **8**. Both parameters (τ_g^{-1}/α) and (σ_{ph}/α) increase linearly with intensity. For CEST **3** (Figure 4b), both (τ_g^{-1}/α) and (σ_{ph}/α) also increase linearly with intensity, and the slope of the photoconductivity line is similar to that for CEST **8**. As eq 3 shows, the slope of (σ_{ph}/α) versus I reflects the product of the charge generation quantum efficiency and the mobility in the simplest model. However, the slope of the speed line for CEST **3** is 1 order of magnitude smaller than for CEST **8**. This result suggests that the speed for CEST **3** is being affected by some other factor, which may be chromophore orientation or some other process. Measurement of the oxidation potentials of the chromophores in the CEST class did not provide a clear trend like that which occurred for the DCST class (data not shown), which is another hint that transport in composites containing the CESTs

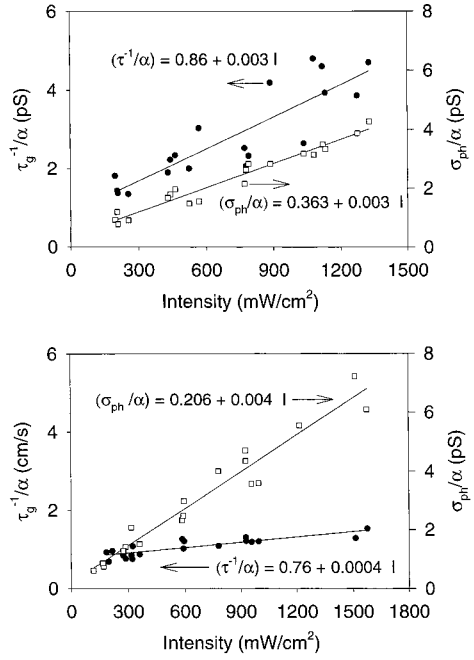

Figure 4. Intensity dependence of the normalized speed ((τ_g^{-1}/α) right axes, open squares) and the normalized photoconductivity ((σ_{ph}/α), left axis, filled circles) of (a) CEST **8** and (b) CEST **3** composites. E = 50 V/μm, λ = 647 nm.

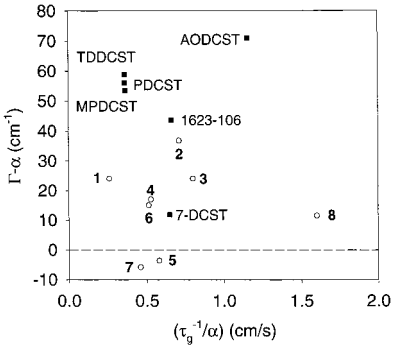

Figure 5. Comparison of the performance of composites of DCST and CEST derivatives. Net gain coefficient versus normalized photorefractive speed (τ_g^{-1}/α). I = 200 mW/cm^2, E = 50 V/μm, λ = 647 nm

is complex. A clear understanding of the role of the different substituents for the CEST class requires further investigation.

A final comparison of the overall performance of composites from the two series of chromophores, DCSTs and CESTs, at 200 mW/cm^2 and 50 V/μm, is illustrated in Figure 5, where the net gain ($\Gamma - \alpha$) is plotted versus the normalized speed (τ_g^{-1}/α). Although both DCSTs and CESTs present very fast response times, the net gain is generally much larger for the DCST derivatives (filled squares). As noted above, this is probably a result of the larger ground-state dipole moment of the DCST derivatives providing higher Pockels and orientational nonlinearity for these chromophores with a dicyano acceptor.

The high speed of these PR polymer composites makes them potentially interesting for video-rate optical processing applications. One way to increase the speed further is to apply higher electric fields, although this might lead to problems of dielectric breakdown. In order investigate this possibility, we performed TWM experi-

Table 3. Photorefractive Properties of Composites of (PVK:chromophore:BBP:C_{60}) for Several DCST and CEST Derivatives at 647 nm, 100 V/μm, and 1 W/cm^2 [a]

chromophore	E (V/μm)	Γ (cm^{-1})	τ_g (ms)	Δn (10^{-3})
AODCST	100	235 ± 76	5 ± 0.8	1.3 ± 0.8
7-DCST	100	130	4	0.8
TDDCST	100	141	14	0.9
CEST **1**	100	74	10	0.7
CEST **2**	100	>140	45	>0.8
CEST **8**	85	55	9	0.5

[a] τ_g (response time, short time constant from double exponential fit) and Δn (refractive index change).

ments at high intensities (1 W/cm^2) and fields (up to 100 V/μm) in some of the compounds. With these experimental conditions, single exponentials did not provide good fits of the gain growth transients, no matter the length of the transient considered in the analysis. We therefore used an alternate fitting function, the sum of two exponentials,

$$\gamma(t) = 1 + a\{1 - \exp[-(t/\tau_1)]\} + b\{1 - \exp[-(t/\tau_2)]\} \quad (4)$$

and then interpreted only the short time constant τ_1. The early time constants (τ_1) obtained from the fits and the steady-state experimental values for Γ and Δn for some of the derivatives are reported in Table 3. Response times as small as 5 ms, while large gain coefficients are maintained (Γ >200 cm^{-1}), were obtained for AODCST. The chromophore 7-DCST showed a 4 ms time constant, but with somewhat reduced gain. Three other materials showed time constants near 10 ms, still useful for video-rate applications. However, at the high fields used, sample breakdown eventually occurred, so further work is required to optimize the sample and electrode preparation protocols to minimize this effect.

Conclusions

In this paper, we have presented the photorefractive properties of polymer composites of the type PVK:chromophore:BBP:C_{60} for two different series of chromophores (DCST and CEST derivatives). These materials show promise for video-rate optical processing applications, since they exhibit response times (τ_g) as small as 60 ms at 50 V/μm and 200 mW/cm^2 and $\tau_g = 5$ ms at 100 V/μm and 1 W/cm^2, while gain coefficients are kept reasonable near 100 cm^{-1}. For the DCST derivatives a clear correlation between the speed and the photoconductivity is observed, which indicates that the speed is dominated by the photoconductivity, rather than by chromophore orientation. In addition, from the measurement of the first oxidation potentials of the chromophores by cyclic voltammetry, it has been shown that the trapping dynamics in these composites is in agreement with a previously reported model which claims that the active trap is C_{60} anion, while the chromophores act as compensating sites. On the other hand, for the CEST derivatives simple correlations between photoconductivity and speed do not exist for all the compounds, suggesting possible limitations by other processes, for example chromophore orientation. Future work should be directed toward clarifying this effect and improving the gain coefficients.

Acknowledgment. We thank Prof. Y. Tor, for assistance with the CV measurements, and M. DeClue, for synthesis of the 7-DCST chromophore. The work at UCSD was supported in part by the U.S. Air Force Office of Scientific Research Grants No. F49620-96-1-0135 and F49620-97-1-0286. The work at KSU was supported in part by the National Science Foundation under Science and Technology Center Advanced Liquid Crystalline Optical Materials grant DMR89-20147.

CM981157H